Proceedings of the 17th World Congress
The International Federation of Automatic Control
Seoul, Korea, July 6-11, 2008

Fault-Tolerant Switching Scheme with Multiple Sensor-Controller Pairs

John J. Martínez [*,1] **María M. Seron** [**] **José A. De Doná** [**]

[*] *Gipsa-lab UMR 5216, Département Automatique. BP.46, St. Martin D'Hères 38440, France (e-mail: Jairo.Martinez@inpg.fr)*
[**] *Centre for Complex Dynamic Systems and Control (CDSC), School of Electrical Engineering and Computer Science, The University of Newcastle, Callaghan, NSW 2308, Australia*

Abstract: This paper deals with the problem of achieving high performance and fault tolerance properties of a given plant by switching between a collection of different sensor-controller pairs. We assume that each sensor-controller pair has been previously designed to achieve an appropriate performance objective according to disturbances, sensor noises, available bandwidth and uncertainties. The proposed strategy selects, at each instant of time, the sensor-controller pair that minimises a suitable switching criterion. Stability of the switching system under normal (fault-free) operation conditions is established in the main result of this paper. In addition, a simulation example of active suspension control illustrates that the proposed switching system is able to maintain performance levels, and to preserve stability under the occurrence of severe faults in some of the sensors.

1. INTRODUCTION

Faults are deviations from a specified mode of behaviour that can take place in different parts of a control system; they can appear in sensors, actuators, or any other component of the system. A fault can be abrupt, intermittent or incipient. Thus, the unpredictable location and characteristic of a fault makes the problem of fault detection a very complex task to be solved.

The problem of fault detection and isolation (FDI) has largely been studied during the last decade and still remains an interesting research topic. The main paradigm consists of first detecting a fault (location and nature) and then, by means of a suitable mechanism, reconfiguring the faulty system in order to maintain its operability (probably accepting a degraded performance). Most of the known approaches for FDI assume knowledge of the possible fault scenario, and then propose control structures that ensure the good behaviour of the system under such faults, see Blanke et al. [2003], Isermann [2005]. Systems that are *tolerant* to faults, that is, systems that continue to perform adequately in the presence of faults, are called fault-tolerant control (FTC) systems.

FTC systems are generally divided into passive-FTC and active-FTC classes. Passive-FTC systems are mainly based on *robust-controller* design techniques and aim at synthesising one robust controller that makes the closed-loop system insensitive to certain faults [Stoustrup and Niemann, 2001, Blanke et al., 2003]. The main advantage of this approach is that it does not require online detection of the faults. However, its applicability is restricted to faults that have a small effect on the behaviour of the system. Hence, increased robustness to certain faults is only possible at the expense of decreased nominal (fault-free) performance.

In the case of active-FTC systems, the main problem concerns the integration of an FDI system together with a particular reconfigurable mechanism which decides the best configuration of the system to achieve fault tolerance. Most of the approaches in the literature are focused on one of both parts—the FDI part or the reconfiguration part—considering that the other part either is absent or behaves perfectly. Indeed, on the one hand many FDI algorithms do not consider the closed-loop operation of the system, and, on the other hand, many FTC reconfigurable mechanisms assume the availability of perfect fault estimates from the FDI scheme. Most of the proposed interconnections do not provide any guarantee of the post-fault performance, or even stability, which can be maintained by such schemes.

In this paper we present a control scheme that tackles the problem of FTC within a new paradigm. This new paradigm consists of using a switching mechanism to implicitly detect the healthy components of the system and automatically reconfigure it to avoid the use of faulty components in closed loop. In addition to this implicit FTC property, the proposed scheme is mainly aimed to maintain high performance of the system during normal (fault-free) operation. The strategy selects, at each instant of time, the suitable sensor-controller pair that provides robust stability. Stability of the switching system under normal (fault-free) operation conditions is established in the main result of this paper. In addition, a simulation example (active suspension control) illustrates that the proposed switching system is able to maintain performance levels, and to preserve stability under the occurrence of severe faults in some of the sensors. Conditions for guaranteing robust stability for different classes of faults are under study.

The control scheme presented here is an extension of that presented in Martínez et al. [2006] and Seron et al. [2007],

[1] Corresponding author. Email: Jairo.Martinez@inpg.fr

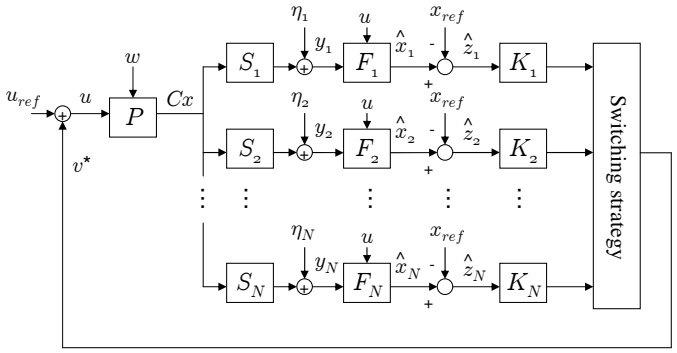

Fig. 1. Multisensor switching scheme with plant P, sensors $S_1, \dots S_N$, estimators $F_1, \dots, F_N$ and feedback gains $K_1, \dots, K_N$.

which was designed for a single control performance objective, that is, using the same feedback gain for all sensor-estimator pairs. In this paper, we consider the use of different feedback gains according to the desired performance for each independent loop, that is, it is assumed that each controller has been designed according to the nature of the corresponding loop disturbances, sensor noises, available bandwidth, uncertainties and actuation constraints. The stability proof established in Martínez et al. [2006], Seron et al. [2007] and Seron et al. [2008], based on a single Lyapunov function for the resulting switched system, is no longer valid for the new scheme, and a new stability proof using multiple Lyapunov functions is then required.

The remainder of the paper is organised as follows. In Section 2 we present and discuss the proposed control scheme. Then, in Section 3, we prove closed-loop stability of the switched system in the presence of bounded disturbances. Finally, in Section 4, an illustrative example is presented, where a quarter active car suspension system affected by different type of disturbances and sensor faults is simulated and discussed.

2. SWITCHING CONTROL SCHEME

In this section we describe the proposed switching control scheme. A schematic of the resulting feedback control system is depicted in Figure 1.

2.1 Problem statement

Consider the following linear discrete-time plant model

$$x^+ = Ax + Bu + Ew, \tag{1}$$
$$y = Cx + Du + Hw, \tag{2}$$

where $x \in \mathbb{R}^n$ and $x^+ \in \mathbb{R}^n$ are, respectively, the current and successor system states, $u \in \mathbb{R}^m$ is the input, $w \in \mathbb{R}^r$ is a bounded process disturbance and $y \in \mathbb{R}^p$ is the output made available to the sensors (see Section 2.2 below). For the system (1) we consider the problem of tracking a state reference signal x_{ref} that satisfies

$$x_{ref}^+ = Ax_{ref} + Bu_{ref}. \tag{3}$$

Assumption 2.1. The pair (A, B) is stabilisable. ◦

Assumption 2.2. The reference signals u_{ref} and x_{ref} in (3) are bounded. ◦

Note that in the case where A has eigenvalues on or outside the unit circle, u_{ref} must be obtained from some stabilising feedback controller for system (3).

We will study the plant tracking error defined as

$$z \triangleq x - x_{ref}. \tag{4}$$

In addition, we define the tracking error for the input as

$$v \triangleq u - u_{ref}. \tag{5}$$

Then, from (1),(3) and (4), the plant tracking error dynamics are described by

$$z^+ = Az + Bv + Ew. \tag{6}$$

In this paper, we assume that the nature of the disturbance w can change with time as a consequence of the system's interaction with its environment. For example, w can change from being a signal with rich harmonic content to a simple low frequency sinusoidal signal (following a changing road profile, for instance, in the case of an active suspension system).

In this context, the tracking problem that we address is to design a control input v such that (i) z is bounded whenever w is bounded and (ii) the sequence $z(k)$ converges to zero as k goes to infinity when so does $w(k)$. In addition, we explore the adaptation of the control objective by means of a switching mechanism so that the bounds on the tracking error remain consistently "small" irrespective of the nature of the disturbance.

2.2 Multi-sensors and Multi-estimators

We assume that the system output (2) is measured via a family of N sensors

$$\xi_i^+ = A_{s_i}\xi_i + B_{s_i}y, \tag{7}$$
$$y_i = C_{s_i}\xi_i + D_{s_i}y + \eta_i, \qquad i = 1, \cdots, N, \tag{8}$$

where, for each sensor, $\xi_i \in \mathbb{R}^{n_i}$ is the state, $y_i \in \mathbb{R}^{p_i}$ is the measured output and $\eta_i \in \mathbb{R}^{p_i}$ is a bounded measurement disturbance.

Assumption 2.3. The matrices A_{s_i} in (7) have all their eigenvalues strictly inside the unit circle. ◦

Assumption 2.4. The pairs

$$\left(\begin{bmatrix} A & 0 \\ B_{s_i}C & A_{s_i} \end{bmatrix}, \begin{bmatrix} D_{s_i}C & C_{s_i} \end{bmatrix} \right)$$

are detectable for $i = 1, \dots, N$. ◦

We consider N state estimators, each of which estimates the states of the series connection of the plant and a sensor. The estimators are described by the following equations, for $i = 1, \cdots, N$:

$$\hat{x}_i^+ = A\hat{x}_i + Bu + L_i(y_i - \hat{y}_i), \tag{9}$$
$$\hat{\xi}_i^+ = A_{s_i}\hat{\xi}_i + B_{s_i}C\hat{x}_i + B_{s_i}Du + L_{s_i}(y_i - \hat{y}_i), \tag{10}$$
$$\hat{y}_i \triangleq D_{s_i}C\hat{x}_i + C_{s_i}\hat{\xi}_i + D_{s_i}Du. \tag{11}$$

Assumption 2.5. The gains L_i, L_{s_i} are such that

$$A_{L_i} \triangleq \begin{bmatrix} A & 0 \\ B_{s_i}C & A_{s_i} \end{bmatrix} - \begin{bmatrix} L_i \\ L_{s_i} \end{bmatrix} \begin{bmatrix} D_{s_i}C & C_{s_i} \end{bmatrix}, \tag{12}$$

for $i = 1, \cdots, N$, have all their eigenvalues strictly inside the unit circle [note that this is always possible by Assumption 2.4] [2]. ◦

[2] If the estimators are steady-state Kalman filters then L_i and L_{s_i} are obtained via an algebraic Riccati equation. More generally, L_i,

Remark 2.6. The estimation errors, defined as

$$\begin{bmatrix}\tilde{x}_i\\ \tilde{\xi}_i\end{bmatrix} \triangleq \begin{bmatrix}x-\hat{x}_i\\ \xi_i-\hat{\xi}_i\end{bmatrix}, \quad i=1,\cdots,N, \tag{13}$$

satisfy, using (1), (7), (8), (9), (10) and (12),

$$\begin{bmatrix}\tilde{x}_i^+\\ \tilde{\xi}_i^+\end{bmatrix} = A_{L_i}\begin{bmatrix}\tilde{x}_i\\ \tilde{\xi}_i\end{bmatrix} + \begin{bmatrix}E-L_iD_{s_i}H\\ B_{s_i}H-L_{s_i}D_{s_i}H\end{bmatrix} w - \begin{bmatrix}L_i\\ L_{s_i}\end{bmatrix}\eta_i. \tag{14}$$

Hence, it follows from Assumption 2.5 that $\tilde{x}_i$ and $\tilde{\xi}_i$ are bounded whenever w and η_i are bounded. ∘

2.3 Multi-controllers

We define the tracking error for the plant state estimates as:

$$\hat{z}_i \triangleq \hat{x}_i - x_{ref}, \tag{15}$$

for $i=1,\cdots,N$.

Then, to each sensor-estimator pair we associate a feedback controller of the form:

$$v_i = -K_i\hat{z}_i, \tag{16}$$

for $i=1,\cdots,N$. Each controller gain K_i is designed independently; for example, in such a way that a certain performance objective is satisfied for the ith plant-sensor-estimator-controller loop. In particular, we assume that K_i is stabilising, that is, the matrix $(A-BK_i)$ has all its eigenvalues inside the unit circle.

Thus, we can always find matrices P_i that satisfy the following condition:

Condition 2.7. Every pair (K_i, P_i) satisfies:

$$(A-BK_i)'P_i(A-BK_i) - P_i \le -Q_i, \tag{17}$$

for $i=1,\cdots,N$, $P_i>0$, $Q_i>0$.

When the controller gain K_i is designed for certain control objectives, for instance H_2 or H_∞ norm minimisation, an associated Riccati equation that implies inequality (17) will be satisfied. For simplicity and generality, we will only use Condition 2.7 in the stability analysis of Section 3.

2.4 Switching strategy

We propose a switching strategy that at each time instant selects a suitable feedback control as follows:

$$v = -K_l\hat{z}_l, \tag{18}$$

for l defined as

$$l \triangleq \arg\min_{i=1,\cdots,N.}\{\hat{z}_i'P_i\hat{z}_i\}, \tag{19}$$

where P_i, $i=1,\ldots,N$, satisfy Condition 2.7.

In the sequel we refer to the index l as the switching signal.

Thus, at each time instant, the switching strategy selects the feedback control (18) that achieves the smallest value $\hat{z}_l'P_l\hat{z}_l$ of the "switching performance criterion" in (19).

3. STABILITY IN PRESENCE OF BOUNDED DISTURBANCES

In this section we prove closed-loop stability of the switching scheme described in Section 2.

L_{s_i} can be computed by placement of the poles of A_{L_i} in some desired location.

From the definitions (4), (13) and (15), the plant tracking error z can be expressed in terms of any estimation tracking error, as

$$z = \hat{z}_i + \tilde{x}_i, \tag{20}$$

for $i=1,\cdots,N$.

Then, to prove the boundedness of z, it is sufficient to prove the boundeness of $\hat{z}_i$ and $\tilde{x}_i$. The estimation errors $\tilde{x}_i$ are bounded by Assumption 2.5. So, we are left with the problem of proving that $\hat{z}_i$ is bounded.

From definition (15), and using (3), (5), (8), (2), (9) and (13), we have:

$$\hat{z}_i^+ = A\hat{z}_i + Bv + \gamma_i, \tag{21}$$

for $i=1,\cdots,N$, where

$$\gamma_i = L_i(D_{s_i}C\tilde{x}_i + C_{s_i}\tilde{\xi}_i + D_{s_i}Hw + \eta_i), \tag{22}$$

which is bounded.

Our main stability result, given in Theorem 1 below, is based on the stability properties of the system (21) in feedback with (18)-(19), that is,

$$\hat{z}_i^+ = A\hat{z}_i + B(-K_l\hat{z}_l) + \gamma_i. \tag{23}$$

Using the fact that, from (20), $\hat{z}_l = \hat{z}_i + (\tilde{x}_i - \tilde{x}_l)$, for all $l,i \in \{1,\ldots,N\}$, the systems (23) can be expressed in terms of $\hat{z}_i$ as follows:

$$\hat{z}_i^+ = (A-BK_l)\hat{z}_i + \gamma_{li}, \tag{24}$$

for $i=1,\ldots,N$, where l is the switching sequence given by (19) and where

$$\gamma_{li} \triangleq -BK_l(\tilde{x}_i - \tilde{x}_l) + \gamma_i. \tag{25}$$

Note that γ_{li} is bounded. Also note that, even though the matrices

$$A_i \triangleq (A-BK_i) \tag{26}$$

have their eigenvalues inside the unit circle, we have to prove the stability of the switched system (24) for any switching signal sequence dictated by (19).

The following theorem establishes stability of the proposed switching control scheme.

Theorem 1. Under Assumptions 2.1 to 2.5, the system (24) in closed loop with the switching control law (18)–(19), has bounded trajectories. Moreover, the plant tracking error (4) and the estimation tracking error (15), for $i=1,\ldots,N$, asymptotically converge to zero in the absence of process and measurement disturbances.

Proof. Consider the family of Lyapunov functions

$$V_i(\hat{z}_i) = \hat{z}_i'P_i\hat{z}_i, \tag{27}$$

for $i=1,\cdots,N$, where $P_i>0$ is as in Condition 2.7. From (17) and (26) we have that the following inequalities are satisfied:

$$\hat{z}_i'A_i'P_iA_i\hat{z}_i - \hat{z}_i'P_i\hat{z}_i \le -\hat{z}_i'Q_i\hat{z}_i, \tag{28}$$

for $P_i>0$, $Q_i>0$, $i=1,\cdots,N$.

Let l_k be the index selected at time k by the switching strategy (19). We then have from (27) that $V_{l_k}(\hat{z}_{l_k}(k)) \le V_i(\hat{z}_i(k))$, for all $i=1,\ldots,N$ and, in particular,

$$V_{l_k}(\hat{z}_{l_k}(k)) \le V_{l_{k-1}}(\hat{z}_{l_{k-1}}(k)), \tag{29}$$

where l_{k-1} is the index selected at the previous time $k-1$ by the switching strategy (19). Also, using (24), (26),

$$\hat{z}_{l_k}(k+1) = A_{l_k}\hat{z}_{l_k}(k) + \gamma_{l_k}(k), \tag{30}$$

where we have used the fact that $\gamma_{li} = \gamma_i$ when $l = i$ [see (25)].

In addition, using (28), (30) and assuming knowledge of a bound [3] $\|\gamma_{l_k}(k)\| \leq \bar{\gamma}_{l_k}$, we have

$$V_{l_k}(\hat{z}_{l_k}(k+1)) \leq V_{l_k}(\hat{z}_{l_k}(k)) + g_{l_k}(\hat{z}_{l_k}(k)), \tag{31}$$

where, for $i = 1, \ldots, N$,

$$g_i(\hat{z}_i(k)) \triangleq -\lambda_m(Q_i)\|\hat{z}_i(k)\|^2 + 2\|\hat{z}_i(k)\|\|A_i' P_i\|\bar{\gamma}_i + \|P_i\|\bar{\gamma}_i^2, \tag{32}$$

and $\|\cdot\|$, $\lambda_m(\cdot)$ denote the 2-norm of a vector and the minimum eigenvalue of a matrix, respectively. Note that

$$g_i(\hat{z}_i(k)) < 0 \quad \text{if and only if } \|\hat{z}_i(k)\| > \rho_i, \tag{33}$$

where

$$\rho_i \triangleq \frac{\|A_i' P_i\| + \sqrt{\|A_i' P_i\|^2 + \lambda_m(Q_i)\|P_i\|}}{\lambda_m(Q_i)}\bar{\gamma}_i.$$

Next, we observe that at least one sensor, say with index j, will be selected infinitely many times by the switching strategy. Let k and $k - r \geq 0$, for some $r \geq 1$, be two time instants at which sensor j is selected, that is, $l_k = j$ and $l_{k-r} = j$. We then have the following two possibilities regarding the satisfaction of condition (33), which result in two different cases for the evolution of the Lyapunov function $V_j(\hat{z}_j)$:

- $\|\hat{z}_{l_{k-i}}(k-i)\| > \rho_{l_{k-i}}$, for $1 \leq i \leq r$, and hence, using (29), (31) and (33) repeatedly we obtain
$$V_j(\hat{z}_j(k)) < V_{l_{k-r}}(\hat{z}_{l_{k-r}}(k-r)) = V_j(\hat{z}_j(k-r)).$$
- $\|\hat{z}_{l_{k-i}}(k-i)\| > \rho_{l_{k-i}}$, for $1 \leq i \leq s-1 < r$, and $\|\hat{z}_{l_{k-s}}(k-s)\| \leq \rho_{l_{k-s}}$. Hence, combining (33) with iterations of (29), and (31) yields
$$\begin{aligned} V_j(\hat{z}_j(k)) &< V_{l_{k-s}}(\hat{z}_{l_{k-s}}(k-s)) + g_{l_{k-s}}(\hat{z}_{l_{k-s}}(k-s)), \\ &\leq \max_{\|\hat{z}\| \leq \rho_{l_{k-s}}} \left[V_{l_{k-s}}(\hat{z}) + g_{l_{k-s}}(\hat{z})\right], \\ &\leq \max_{i \in \{1,\ldots,N\}} \left\{ \max_{\|\hat{z}\| \leq \rho_i} \left[V_i(\hat{z}) + g_i(\hat{z})\right] \right\}. \end{aligned}$$

Note that the quantity on the right hand side above is bounded since both functions V_i and g_i are continuous.

Thus, the Lyapunov function $V_j(\hat{z}_j)$ either decreases between times when sensor j is selected, or is bounded at the times when sensor j is selected. Moreover, in between those instants, the state $\hat{z}_j(k)$ evolves with the bounded dynamics (24) during a finite number of steps. [4] We conclude that the state $\hat{z}_j(k)$ is bounded for all $k \geq 0$.

In addition, any other tracking error subsystem trajectories (even if the corresponding sensor is never chosen) are also bounded because the following property always holds:

$$z = \hat{z}_i + \tilde{x}_i = \hat{z}_j + \tilde{x}_j, \tag{34}$$

for $i, j = 1, \cdots, N$. Property (34) also shows that the plant tracking error z is bounded whenever $\hat{z}_i$ and $\tilde{x}_i$ are bounded and converges to zero if $\hat{z}_i$ and $\tilde{x}_i$ converge to zero. This completes the proof of the theorem. □

[3] Such bounds can be obtained from (14) and (22) assuming knowledge of bounds on the process and measurement disturbances.

[4] Alternatively, one can argue that, by a similar analysis, the tracking error states of all sensors chosen between the times at which sensor j is selected are bounded at the times when they are selected. Hence, the relation $\hat{z}_j = \hat{z}_i + (\tilde{x}_i - \tilde{x}_j)$, for all $i, j = 1, \ldots, N$, together with bounds on the estimation errors prove boundedness of the state $\hat{z}_j(k)$ between its selection times. This alternative argument also yields a computable bound estimate on the tracking error states.

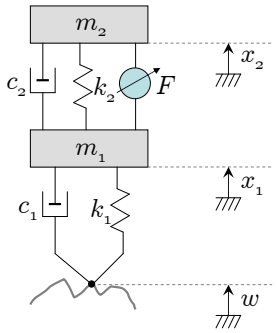

Fig. 2. Active suspension system.

4. ILLUSTRATIVE EXAMPLE

In this section we apply the proposed switching scheme to a simulation example of vehicle active suspension control.

4.1 Active-suspension system description

We consider the synthesis of active controllers for a suspension system similar to that described in Poussot-Vassal et al. [2006]. We consider the rear wheel of a tractor-trailer combination as depicted in Figure 2. Here, m_1 represents tire, wheel and rear axle mass, and m_2 denotes a fraction of the semitrailer mass. The deflection variables x_2, x_1 and w are properly scaled so that $x_2 - x_1 = 0$ and $x_1 - w = 0$ in steady state.

The system is modeled by the state space equations

$$x^+ = Ax + Bu + Ew, \tag{35}$$

which correspond to the discretisation of the continous time system with a sample time of $10ms$. The disturbance signal w (road profile), is modeled as a sinusoidal signal with magnitude W, frequency Ω, and phase ϕ, that is,

$$w(t) = W \cdot \sin(\Omega \cdot t + \phi), \ \forall t > 0. \tag{36}$$

We have simulated the disturbance (36) with the following values: $W = 0.01m$, $\Omega = 2\pi f$ with $(f = 3Hz)$ and $\phi = 0$. The model parameters values and the respective matrices are presented in Appendix A.

The state of the system is defined (in continuous time) as follows: $x = [x_1 \ x_2 \ \dot{x}_1 - b_1 w/m_1 \ \dot{x}_2]'$ and the states that form part of the output equation (2) are $[\ddot{x}_2 \ \ x_2 - x_1]'$. The control input is the force $u = F$ and the exogenous disturbance input is the road profile w. The sensor models are assumed to have no dynamics and are described as follows:

$$y_i = y + \eta_i = Cx + Du + Hw + \eta_i, \qquad i = 1, \cdots, N. \tag{37}$$

We assume the availability of two different controllers which assure the stability of the closed-loop system. The controllers are previously designed to achieve low levels of vertical acceleration ($\ddot{x}_2$), bounded suspension deflection ($x_2 - x_1$ and $x_1 - w$) and bounded dynamic tire force (F). The estimators are suitable filters designed as in Section 2.2, and the controllers are particular feedback gains obtained by LQR methods. One of the controller only penalises the states deviations, while the second one

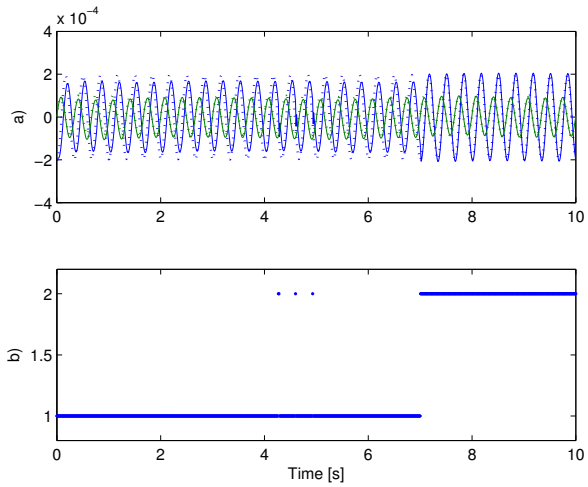

Fig. 3. a) State trajectories (solid line) and reference trajectories (dotted line), and b) The switching sequence.

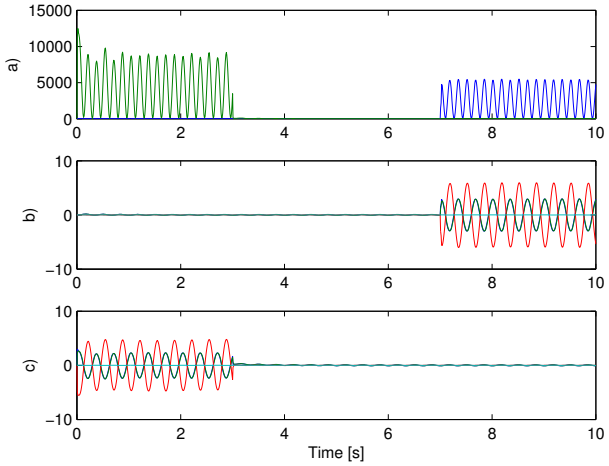

Fig. 4. a) Cost functions $\hat{z}_i' P_i \hat{z}_i$ during failures: sensor 2 (*left*) and sensor 1 (*right*), b) Estimation errors from sensor 1, and c) Estimation errors from sensor 2. Both non available in practice.

penalises both the state deviations and the control effort with same weight. The controller gains K_1 and K_2, and resulting eigenvalues achieved for each loop are given in Appendix A. Also given in Appendix A are the associated cost function matrices P_1 and P_2, obtained from the Riccati equations corresponding to each LQR controller, which are used in the switching strategy (19). Note that the controller gains and cost function matrices satisfy Condition 2.7 and thus closed-loop stability in the absence of failure is guaranteed by Theorem 1.

4.2 Sensor-failure scenario

Here, we consider abrupt faults that lead to a sensor outage. In the moment of a sensor fault, its output does not provide information about states, and only produces a noise signal (possibly with higher variances), i.e., when the j sensor fails, its measured output during the fault is given by:

$$y_j = \eta_j^F,$$

where η_j^F is a bounded noise. We also consider the recovery of a sensor after a fault, that is, when it measured output instantly reverts to (37). The simulated scenario concerns, firstly, a failure in sensor-2 at 0 seconds, and its recovery at 3 seconds. Sensor 1 is healthy from 0 to 7 seconds, time when it fails. Thus, only during the period of 3 to 7 seconds both sensors work perfectly (fault-free operation). The switching sequence (chosen controller) is obtained by the strategy described in Section 2.4.

Figure 3 illustrates the dynamic behavior of the switched system. In particular, Figure 3a shows the state values (solid lines), which track the state references (dotted curves). We remark that the state signals are not affected by the controller switching and the performance remains within acceptable values (according to the chosen controller).

Figure 4a depicts the cost function values for each sensor. Figures 4b and 4c, show the estimation errors (accessible only in simulation) and Figures 5a and 5b the tracking errors. From these figures we observe that the high cost function values are well correlated with the high estimation

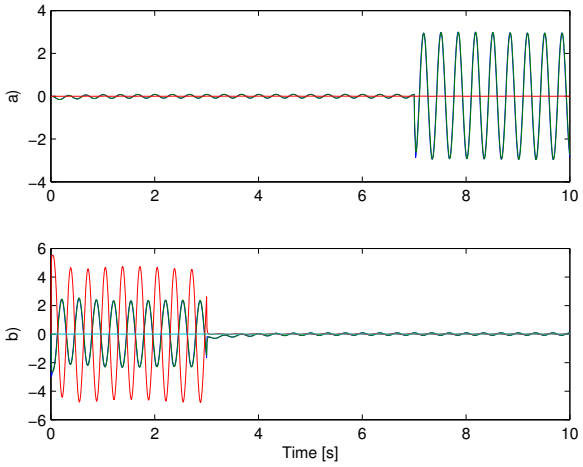

Fig. 5. a) Tracking errors from sensor 1, and b) Tracking errors from sensor 2. Both available in practice.

errors and the tracking errors due to the faulty sensor. The following equation, from (34), could explain this behavior.

$$\begin{aligned} \hat{z}_i &= z - \tilde{x}_i, \\ \hat{z}_j &= z - \tilde{x}_j, \end{aligned} \tag{38}$$

for $i = 1, \cdots, N$, $j \neq i$. Thus, during a sensor failure, for sufficiently small values of z, the estimation error magnitudes $\tilde{x}_i$ (always unmeasurable in practice), are mostly described by the tracking error magnitudes. This aspect suggests that there may exist system conditions (system parameters, noise levels, estimation errors, etc.) to guarantee the selection of healthy sensors that will assure the stability of the switching system during failures.

The conditions for the switching controller to always choose a healthy sensor to close the loop, or even for admitting to choose a faulty sensor at particular times without affecting stability of the system are under investigation.

The previous figures illustrate the stabilising role of the switching strategy during failures. However, we may be

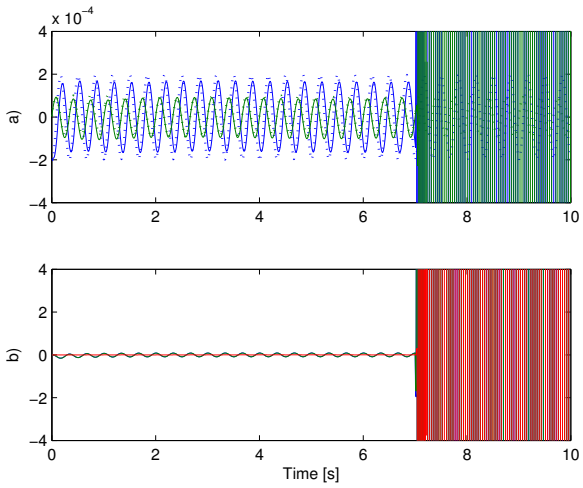

Fig. 6. Failure scenario using only sensor 1 (i.e. without switching); here sensor 1 fails at 7 seconds. a) State trajectories (solid line) and reference trajectories (dotted line), and b) estimation errors from sensor 1.

interested in observing the performance of the system without the switching strategy. Figure 6 illustrates the behaviour of the system in closed loop with only one sensor-controller pair (the first sensor and its associated controller), that is, without using the switching strategy. Sensor 1 fails at 7 seconds and we can observe, as expected, that the closed-loop system becomes unstable.

5. CONCLUSIONS

In this paper, we have presented a novel control switching scheme which selects at each time instant a controller (from a bank of different controllers) in such a way that the stability of the closed-loop system is guaranteed. The proposed scheme presents interesting properties in terms of both fault-free performance and fault-tolerance.

Faulty sensor detection and isolation is achieved "implicitly" by guaranteeing that the switching cost avoids selecting faulty sensors. This is the main feature of the proposed strategy, which departs from other available techniques. The on-line implementation of the scheme is simple, requiring only to compare cost values. The stability properties during different classes of failures are under study.

Appendix A. SIMULATION PARAMETERS

The following table summarises the parameter values of the active suspension model used during simulations:

Parameter values				
m_1	59	m_2	290	(Kg)
k_1	19e4	k_2	16812	(N/m)
c_1	34	c_2	1000	$(N/m/s)$

The matrices A, B, E, C, D, and H of the continuous time model (before discretisation) are described as follows:

$$A = \begin{bmatrix} 0 & 0 & 1 & 0 \\ 0 & 0 & 0 & 1 \\ -k_1 + k_2/m_1 & k_2/m_1 & -c_1 + c_2/m_1 & c_2/m_1 \\ k_2/m_2 & -k_2/m_2 & c_2/m_2 & -c_2/m_2 \end{bmatrix}, \quad \text{(A.1)}$$

$$[B\ E] = \begin{bmatrix} 0 & c_1/m_1 \\ 0 & 0 \\ -1/m_1 & (k_1/m_1) - (c_1(c_1+c_2))/(m_1 m_1) \\ 1/m_2 & c_1 c_2/m_1 m_2 \end{bmatrix}, \quad \text{(A.2)}$$

$$C = \begin{bmatrix} \frac{k_2}{m_2} & -\frac{k_2}{m_2} & \frac{c_2}{m_2} & -\frac{c_2}{m_2} \\ -1 & 1 & 0 & 0 \end{bmatrix}, \quad \text{(A.3)}$$

$$[D\ H] = \begin{bmatrix} \frac{1}{m_2} & \frac{c_1 c_2}{m_1 m_2} \\ 0 & 0 \end{bmatrix}. \quad \text{(A.4)}$$

The discrete version of the system is obtained by using the Bilinear (Tustin) approximation, and a sample time of $10ms$. The feedback gains used for each loop are:

$$K_1 = 1.0e3 \cdot [-0.9907\ 0.8327\ -0.9205\ 3.0363],$$

$$K_2 = 1.0e3 \cdot [-0.1463\ 0.1883\ -0.3173\ 1.1963],$$

achieving the following closed-loop eigenvalues for K_1: $0.9903 \pm 0.0171i$, $0.9963 \pm 0.0039i$; and for K_2: $0.9968 \pm 0.0185i$, $0.9982 \pm 0.0028i$. Matrices A_d and B_d are the corresponding matrices of the discrete system (A_d, B_d, C_d, D_d) obtained from the continuous model (A.1)-(A.4). The cost function matrices P used for performing the switching law (19) are:

$$P_1 = 1.0e3 \cdot \begin{bmatrix} 0.3434 & -0.0949 & -0.0060 & -0.3256 \\ -0.0949 & 0.3129 & 0.0366 & 0.4251 \\ -0.0060 & 0.0366 & 0.0724 & 0.0843 \\ -0.3256 & 0.4251 & 0.0843 & 1.3059 \end{bmatrix},$$

$$P_2 = 1.0e3 \cdot \begin{bmatrix} 0.7639 & -0.1158 & 0.0039 & -0.4243 \\ -0.1158 & 0.4326 & 0.0269 & 0.6834 \\ 0.0039 & 0.0269 & 0.2054 & 0.0842 \\ -0.4243 & 0.6834 & 0.0842 & 3.8980 \end{bmatrix}.$$

The estimators were designed according to Section 2.2. The estimation error dynamics is mainly described by the eigenvalues of the matrix A_{L_i}, in equation (2.5). We have chosen the following eigenvalues: 0.000951, 0.360515, 0.983325, 0.999983. For simplicity, we have used the same estimator design for both sensors.

REFERENCES

M. Blanke, M. Kinnaert, J. Lunze, and M. Staroswiecki. *Diagnosis and Fault-Tolerant Control*. 2003.

R. Isermann. *Fault-Diagnosis Systems: An Introduction from Fault Detection to Fault Tolerance*. 2005.

J.J. Martínez, X.W. Zhuo, J.A. De Doná, and M.M. Seron. Multisensor switching strategy for automotive longitudinal control. In *Proc. of the 2006 American Control Conference*, Minneapolis, MN, USA, 2006.

C. Poussot-Vassal, O. Sename, L. Dugard, P. Gáspár, Z. Szabó, and J. Bokor. Multi-objective qLPV $\mathcal{H}_\infty/\mathcal{H}_2$ control of a half vehicle. In *In: Proc. of the Mini conference on Vehicle System Dynamics, Identification and Anomalies (VSDIA)*, Budapest, Hungary, 2006.

María M. Seron, Xiang W. Zhuo, José A. De Doná, and John J. Martínez. Multisensor switching control strategy with fault tolerance guarantees. *Automatica*, 44(1):88–97, 2008.

M.M. Seron, X.W. Zhuo, J.A. De Doná, and J.J. Martínez. Fault tolerant multisensor switching control strategy. *European Control Conference*, 2007.

J. Stoustrup and H. Niemann. Fault tolerant feedback control using the youla parametrization. *In: Proc. of the 6th European Control Conference. Porto*, 2001.